



# Purifying, cloning and characterizing a novel dehalogenase from *Bacillus* sp. GZT to enhance the biodegradation of 2,4,6-tribromophenol in water<sup>☆</sup>



Zhishu Liang<sup>a, c</sup>, Guiying Li<sup>b</sup>, Taicheng An<sup>a, b, \*</sup>

<sup>a</sup> State Key Laboratory of Organic Geochemistry and Guangdong Key Laboratory of Environmental Protection and Resources Utilization, Guangzhou Institute of Geochemistry, Chinese Academy of Sciences, Guangzhou 510640, China

<sup>b</sup> Guangzhou Key Laboratory of Environmental Catalysis and Pollution Control, School of Environmental Science and Engineering, Institute of Environmental Health and Pollution Control, Guangdong University of Technology, Guangzhou, 510006, China

<sup>c</sup> University of Chinese Academy of Sciences, Beijing 100049, China

## ARTICLE INFO

### Article history:

Received 24 December 2016

Received in revised form

6 March 2017

Accepted 18 March 2017

### Keywords:

2,4,6-Tribromophenol

Dehalogenase

Biodegradation

*Bacillus* sp. GZT

## ABSTRACT

2,4,6-Tribromophenol (TBP), an intermediate of brominated flame retardants, can easily release to environment and recalcitrant to degradation. Previously, *Bacillus* sp. GZT, a pure aerobic strain capable of simultaneously debrominating and mineralizing TBP, was successfully isolated by us. To further obtain a practical application and dig up its TBP degradation mechanism, a total of 46.7-fold purification of a novel dehalogenase with a final specific activity of 18.9 U mg<sup>-1</sup> and a molecular mass of 63.4 kDa was achieved. Under optimal conditions (35 °C and 200 rpm), up to 80% degradation efficiencies were achieved within 120 min. Adding H<sub>2</sub>O<sub>2</sub>, NADPH, Mn<sup>2+</sup> and Mg<sup>2+</sup> promoted enzyme reaction effectively; while EDTA, methyl viologen, Ni<sup>2+</sup>, Cu<sup>2+</sup>, Ca<sup>2+</sup> and Fe<sup>2+</sup> strongly inhibited reaction activities. The debromination of TBP was catalyzed by the enzyme at a *K<sub>m</sub>* of 78 μM and a *V<sub>max</sub>* of 0.65 min<sup>-1</sup> mg protein<sup>-1</sup>, which indicated that this dehalogenase could specifically eliminate TBP with a high efficiency and stability. Based on MALDI-TOF/TOF analysis, the dehalogenase shared 98% identity with peptide ABC transporter substrate-binding protein. One open reading frame (ORF) encoding this peptide was found in Strain GZT genome, subjected to clone and expressed in *Escherichia coli* (*E. coli*) to characterize the encoding gene. Result showed that this recombinant strain could also remove as similar amount of TBP as *Bacillus* sp. GZT under the identical condition. Based on these results, we suggest that this newly-isolated TBP dehalogenase highlights a new approach for remediating TBP pollution.

© 2017 Elsevier Ltd. All rights reserved.

## 1. Introduction

Brominated flame retardants (BFRs) constitute a large group of environmental pollutants. For example, 2,4,6-tribromophenol (TBP), a reactive intermediate of the widely used BFR tetrabromobisphenol-A (TBBPA), has been used extensively to prevent fire in the electronic devices including televisions, computers, thermoplastic polyesters, epoxy resins, and polystyrene

(Weidlich et al., 2013). TBP is also used as a pesticide and wood preservative in industry manufacturing (Li et al., 2015; Zu et al., 2013).

Unfortunately, with an annual global use of over 23,000 tons in 2003 (Contreras et al., 2009), TBP has been frequently detected in various environmental matrices, including water, air, dust, sediments and soil (Xiong et al., 2016). It has also been found in fish, and in the plasma of people producing electronics dismantlers and circuit boards at concentrations ranging from 0.17 to 81 ng g<sup>-1</sup> fat (Ezechias et al., 2014; Thomsen et al., 2001). TBP was classified as a hazardous waste by the United States Environmental Protection Agency (USEPA) in 1998 (Li et al., 2015). There is significant evidence that TBP causes adverse effects when released into the environment. For example, TBP can affect thyroid hormone systems in animals and humans (Weidlich et al., 2013; Yamada et al., 2008),

<sup>☆</sup> This paper has been recommended for acceptance by Prof. von Hippel Frank A.

\* Corresponding author. Guangzhou Key Laboratory of Environmental Catalysis and Pollution Control, School of Environmental Science and Engineering, Institute of Environmental Health and Pollution Control, Guangdong University of Technology, Guangzhou, 510006, China.

E-mail address: [antc99@gdut.edu.cn](mailto:antc99@gdut.edu.cn) (T. An).

and it exhibits developmental neurotoxicity, embryotoxicity, and fetotoxicity in some mammals (Zu et al., 2013). Recent investigations found that TBP exposure was associated with an acute oral LD<sub>50</sub> of 1995 and 1819 mg kg<sup>-1</sup> body weight in males and females rats, respectively (Ezechias et al., 2014). Given the rising demand for TBP, increasing TBP contamination is expected in the future. As such, it is critical to better describe its environmental fate, and develop cost-effective treatment or remediation approaches.

Microorganisms are the major mediators for BFR cycling in the environment, because they gain energy by coupling dehalogenation of halogenated compounds to electron transport coupled phosphorylation. This is done through a chemical reaction called dehalorespiration (Futagami et al., 2008). This reaction involves replacing one halogen atom with other atom, making the contaminants significantly more biodegradable (Luo et al., 2011). As such, some studies have reported several cultures or strains capable of the reductive debromination of TBP. These include synthetic microbial community consisting of *Clostridium* sp. Ma13, *Dehalobacter* sp. phylotype FTH1, and *Desulfatiglans parachlorophenolica* DS (Li et al., 2015). *Ochrobactrum* sp. TB01 (Yamada et al., 2008), *Achromobacter piechaudii* (Ronen et al., 2000), *Bacillus* sp. GZT (Zu et al., 2012), and fungi *Trametes versicolor* (Donoso et al., 2008).

Biodegrading BFRs into harmless products relies on the catabolic dehalogenases (DHAs) in these microorganisms, which catalyze the conversion of substrates into different products by providing favorable conditions with lower reaction activation energy (Karigar and Rao, 2011; Parthasarathy et al., 2015). Based on the way DHA cleaves the halogenated pollutant, DHAs can be classified as three categories including hydrolytic, reductive and oxygenolytic ones, which could perform dehalogenation by the replacement of the halogen atom in the aromatic ring with the hydroxyl group from water, hydrogen atom from H<sub>2</sub> and hydroxyl group from O<sub>2</sub>, respectively (Arora and Bae, 2014).

However, the current understanding of DHAs capable of degrading halogenated compounds is limited to studies with relative few purified enzymes. Except for the enzyme responsible for the degradation of 2,4-D and 2,4,5-T (Travkin et al., 1999) and haloalkanes (Janssen et al., 2005), most of these have been biochemically characterized as reductive dehalogenases (RDases). These RDases included PceA, TceA, CrdA, CprA, and VcrA, which can dehalogenation of tetrachloroethene, trichloroethene, trichlorophenol, chlorophenol, and vinyl chloride, respectively (Jugder et al., 2016; Parthasarathy et al., 2015; Schmidt et al., 2014). These RDases are found primarily in the well-studied anaerobic organisms, including *Dehalococcoides*-, *Sulfurospirillum*-, *Dehalobacter*-, *Desulfotobacterium*-, *Shewanella*- and *Desulfomonile*-type microorganisms (Chow et al., 2010; Lohner and Spormann, 2013; Parthasarathy et al., 2015). The first biochemically characterized RDase was 3-chlorobenzoate RDase from *Desulfomonile tiedjei* DCB-1 (Ni et al., 1995). The most extensively studied RDases were from *Dehalococcoides* strain CBDB1 with a total of 32 putative RDases identified in its complete genome sequence (Morris et al., 2007). Besides, under aerobic conditions, enzymes involved in degrading dehalogenating compounds, such as 4-chlorobenzoyl-CoA-, 4-chlorobenzoate-, chlorothalonil- and atrazine chlorohydrolyase-hydrolytic DHAs; 2,5-dichlorohydroquinone-, tetrachlorohydroquinone- and 4-chloro-2-aminophenol-RDases, have also been molecularly characterized from several contaminant degrading bacteria (Arora and Bae, 2014). Despite this previous research, little is known about the DHAs or enzymes involved in the dehalogenation of brominated compounds in aerobes. Only few papers have reported the purification of the enzymes capable of biodegrading brominated aromatics, including dehaloperoxidase and laccases (Chen et al., 2013; Modaressi et al., 2005; Uhnakova

et al., 2009). No published works have addressed enzymes which can effectively decontaminate TBP, although TBP debromination by various microorganisms has been reported. This lack of research has hindered the further identification and development of strains and functional enzymes that could contribute to remediate TBP-contaminated environments.

Recently, our research group isolated the pure aerobic strain, *Bacillus* sp. GZT, which is capable of simultaneously debrominating and mineralizing TBP (Zu et al., 2012). However, its functional enzymes have not yet been investigated. Therefore, this study focused on determining the role of dehalogenase in the GZT strain in TBP degradation, and investigating the molecular mechanism of TBP metabolism. First, a novel DHA-specific enzyme from the GZT strain was purified. Followed by gene cloning and expression to demonstrate the encoding gene, the dependence of debrominase activity on the removal efficiency by this enzyme was investigated. Next, the parameters that most impact TBP biodegradation and mineralization in aerobes were optimized, including substrate concentrations, initial pH, temperature, and metal ion addition. Finally, the main intermediates were identified, and the fate of TBP in this enzyme reaction solution under oxic conditions was explored. This study is the first example of the dehalogenase catalyzed debrominating of TBP, and as such, may support a deeper understanding of the enzyme process that contributes to TBP attenuation at contaminated sites.

## 2. Materials and methods

### 2.1. Chemicals, strain and growth medium

The chemicals used in this study and the detailed recipes for the strain culture medium are provided in the Supporting Information (SI). The strain *Bacillus* sp. GZT (GZT strain) was previously isolated from the sludge of an electronic waste recycling site, using TBP as the sole carbon and energy source (Zu et al., 2012). A pure culture of the GZT strain was grown at 37 °C in 100/250 mL liquid medium. The cells were centrifugally harvested in the late-exponential growth phase for 10 min at 8000 g at 4 °C. The cell pellet was then washed and transferred into 100 mL mineral medium containing 6 mg L<sup>-1</sup> TBP at 37 °C, pH 7.0, and 200 rpm shaking for the incubation.

### 2.2. Preparation of crude extract

After inducing DHA expression by TBP for 120 h, cell pellets were centrifugally harvested for 10 min at 8000 g at 4 °C and washed twice with 20 mM Tris-Cl, pH 7.5. The supernatant designated as the extracellular enzyme was retained and concentrated by ultrafiltration with an Amicon Ultra-15 Centrifugal Filter Unit with Ultracel-10 membrane (Millipore). The concentrated cells were stored frozen at -80 °C, followed by thawed on ice and re-suspended in 20 mM Tris-Cl (pH 7.5; 10 mL per 1 g pellet) containing 50 mg L<sup>-1</sup> lysozyme and 1 mM dithiothreitol. Then, the cells were broken on ice using sonication at 20% power for 180 cycles. Each cycle included 5 s pulse and 5 s cooling periods. The suspension was stirred on ice for 30 min to solubilize the pellet. Subsequently, the lysate was centrifuged at 13000 g for 20 min at 4 °C, and the supernatant was obtained as intracellular crude extract. The pellet, containing the total membrane proteins, was again suspended into 10 mL of 20 mM Tris-Cl, containing 1 mM dithiothreitol and 20% (v/v) glycerol, and stored at -80 °C. Followed by thawing on ice and adding 0.1% Triton X-100, the crude membrane fraction was agitated for 45 min at 4 °C and centrifuged at 13,000 g for 30 min at 4 °C. The supernatant was used to further characterize the enzyme activity involved in biodegrading the TBP.

All fractions, including extracellular enzyme, intracellular crude extract and membrane protein, were assayed for dehalogenase activity.

### 2.3. Ammonium sulfate fractionation

The crude enzyme with the highest dehalogenase activity was fractionated by incrementally adding crystalline ammonium sulfate to reach 40, 60 and 80% saturation levels with constant stirring; all purification steps were performed at 4 °C. At the 40% saturation level, the precipitation was centrifugally collected at 13000 g for 30 min and dissolved in buffer A (20 mM Tris-Cl, pH 7.5, 1 mM dithiothreitol); the supernatant was used to reach a 60% saturation level with additional  $(\text{NH}_4)_2\text{SO}_4$ . Following centrifugation, the precipitate was also collected and dissolved in buffer A. The same method was then used to reach a 80% saturation level. All fractions were assayed for TBP biodegradation activity; the 40–60% precipitation fraction, containing the highest TBP biodegradation activity, was dialyzed twice overnight against buffer A. This was done to remove  $(\text{NH}_4)_2\text{SO}_4$  using Spectra/Por<sup>®</sup> Biotech Dialysis Membranes (MWCO = 10 kDa). Finally, the enzyme solution was concentrated using ultrafiltration.

### 2.4. Partial purification of TBP dehalogenase

A sample of 40 g DEAE-cellulose matrix was added as a slurry in buffer A; the sample was allowed to gravitationally settle to approximately 42 mL. All the buffer and protein samples were filtered through a 0.45  $\mu\text{m}$  filter. The concentrated enzyme solution was applied to DEAE-cellulose column (1.6  $\times$  50 cm) pre-equilibrated with 5 column volumes of buffer A. After washing with 210 mL of buffer A at a flow rate of 5 mL min<sup>-1</sup>, the column was then eluted with 5 column volumes of a linear gradient of NaCl ranging from 0 to 0.5 M in the buffer A. All the peaks with protein were collected to allow for the separate analysis of dehalogenase activity. At 0–0.35 M NaCl gradient, the bound proteins were eluted and shown to have TBP biodegradation activity. The sample was then concentrated and desalted through ultrafiltration, and the TBP-degrading enzyme elution was again loaded onto the same DEAE-cellulose column. The column was regenerated using the procedure in SI and equilibrated with buffer A. Then, the column was washed with buffer A using the same process described above and eluted with 210 mL of a linear gradient mix of 0–0.35 M NaCl in buffer A at 0.25 mL min<sup>-1</sup>. Fractions were again assayed to assess dehalogenase activity. Subsequently, the active fractions, found at 0.25 M NaCl, were pooled and concentrated using ultrafiltration (Fig. S1).

### 2.5. Complete purification of enzyme and dehalogenase activity assays

The enzyme was further purified using gel filtration with a Sephadex G-150 column (1.0  $\times$  40 cm). The column was pre-equilibrated with potassium phosphate buffer (20 mM, pH 7.5, 1 mM dithiothreitol), then eluted with the same buffer at 2 mL min<sup>-1</sup>. The peak with the highest dehalogenase activity was pooled and frozen at -20 °C for future use (Fig. S1). All the enzyme activity experiments were conducted using 3 mL standard mixtures (50 mM Tris-Cl, pH 7.5, 6 mg L<sup>-1</sup> TBP and 1 mM H<sub>2</sub>O<sub>2</sub>), and were performed in triplicate in a 12 mL volume culture tube stoppered with dual cap. The reaction was started by adding 50  $\mu\text{L}$  of the prepared enzyme. After 2 h incubation at 35 °C, 200 rpm, the reaction was terminated by adding 0.2 M NaOH to adjust the pH to 9.0–10.0. The mixture was then boiled for 5 min.

Control experiments were conducted under identical

experimental conditions as described above, except no enzyme was used. The solution was subsequently centrifuged for 10 min at 13000 g and filtered through a 0.22  $\mu\text{m}$  filter (Shanghai ANPEL, China). The remaining TBP in the mixture was determined using high-pressure liquid chromatography (HPLC) as described below. One unit of TBP dehalogenase activity is defined as the amount of enzyme that can catalytically eliminate 1  $\mu\text{M}$  TBP per minute. The specific activity was expressed as units per milligram protein; the activity was calculated after each purification step. Protein concentrations were measured using a Bradford Protein Assay Kit with Serum Albumin as the standard. All the experiments were performed independently; the presented results are the average values of data obtained from triplicates.

### 2.6. Molecular mass estimation and protein identification

The molecular mass and protein purity of the enzyme preparation were estimated using sodium dodecyl sulfate-polyacrylamide gel electrophoresis (SDS-PAGE), with 10% separating gels and 5% stacking slab gels according to reference (Laemmli, 1970). Before electrophoresis, the protein samples were mixed with protein gel loading buffer containing SDS, and boiled at 100 °C for 3 min. Then, a 30  $\mu\text{L}$  sample was loaded in preformed wells. The process was run at 100 V for 30 min, and then run at 120 V for 40 min. Following the separation, the protein bands were visualized by staining the sample with Coomassie brilliant Blue R-250. The gel was then excised and digested with trypsin using ProteasMAX surfactant for in-gel protein digestion. This enabled further identification of the proteins.

Finally, a Proteomics Analyzer Matrix-assisted laser desorption/ionization mass spectrometry with automated tandem time-of-flight fragmentation of selected ions (MALDI-TOF/TOF MS) was used to identify the component protein homologs in each excised band. Proteins were identified based on the combined MS and MS/MS spectra using a 95% or higher confidence interval ( $p > 0.5$ ). Peptide mass fingerprints and MS/MS spectra for each sample were combined and searched for in the Swiss-Prot database and the NCBI's non-redundant database. Search parameters were set to 100 ppm and 0.5 Da error tolerance for MS and MS/MS spectra, respectively. Variable modifications included the allowance for one missed trypsin cleavage, methionine oxidation, and carbamido-methylated cysteine.

### 2.7. Cloning and expression of TBP dehalogenase gene

To further identify the gene encoding the enzyme corresponding to TBP degradation, the cloning and expression of this gene in the *E. coli* has been investigated based on the described method in the reference (Su et al., 2014). To be specific, the gene coding for TBP dehalogenase was amplified by PCR with genomic DNA of *Bacillus* sp. GZT as a template. The primers sequences carrying BamHI and XhoI restriction sites were designed according to the genomic sequence as follows: 5'-CGGGATCCGTGACGGCAAAGGGAAGAG-3' and 5'-CCCTCGAGGATTATATCCACCTTAGACC-3'. This PCR fragment was ligated into the T site of the pMD<sup>™</sup>19-T Vector, and transformed into competent *E. coli* DH5a. After plated onto Luria-Bertani (LB) agar plates containing ampicillin, IPTG and X-gal, and incubated overnight, white colonies were screened and further sequenced. Then, the targeted fragments digested by the restriction enzymes BamHI/XhoI were recovered and ligated into the BamHI/XhoI sites of pET30a (+) vector to generate recombinant plasmid pET-tbp.

For the expression, the recombinant plasmid was transformed into competent *E. coli* BL21 (DE3). Colonies with the ability to use TBP as carbon and energy source were selected and further

confirmed by PCR amplification and sequencing using the primers described above. The sequence of TBP dehalogenase gene has been deposited at GenBank under accession number KY065446. *E. coli* BL21 (DE3) cells, harboring plasmid pET-tbp were grown at 30 °C in LB containing 30 µg mL<sup>-1</sup> kanamycin. The synthesis of TBP dehalogenase was induced by the addition of 1 mM IPTG when OD<sub>600</sub> was set approximately 0.6. One to three hours after the induction, all cells were harvested by centrifugation, re-suspended in a 50 mM potassium phosphate buffer (pH 7.5), and disrupted by ultrasonic oscillation. Then the final preparation of the enzyme was visualized by SDS-PAGE.

### 2.8. Biochemical characterization of TBP dehalogenase

The optimum pH, pH stability as well as the effects of different metal ions (Mg<sup>2+</sup>, Ni<sup>2+</sup>, Ca<sup>2+</sup>, Cu<sup>2+</sup>, Zn<sup>2+</sup>, Mn<sup>2+</sup> and Fe<sup>2+</sup>) and other reagents (H<sub>2</sub>O<sub>2</sub>, glutathione, EDTA and methyl viologen) on the enzyme activity of purified dehalogenase were investigated under standard conditions based on the method described in the SI.

Furthermore, the substrate specificity of the purified enzyme was also determined by assaying the enzyme activity toward different halogenated substrates. The reaction mixture was performed under standard conditions, and with the separately addition of 6 mM 2,4-dibromophenol (2,4-DBP), 2,6-DBP, benzoic acid, phenylacetic acid, 2-bromophenol (2-BP), 4-BP, 3-BP, 2,6-dibromo-4-methylphenol, phenol, or 1,3-dibromo-2-methoxy-5-methylbenzene. The kinetic parameters,  $K_m$  (Michaelis constant) and  $V_{max}$  (maximum velocity), for TBP degradation by the enzyme were determined from Lineweaver-Burk double reciprocal plot with TBP concentrations in the range of 15–75 µM, using the following equation and the computer program:  $\frac{1}{v} = \frac{K_m}{V_{max}} \cdot \frac{1}{[C]} + \frac{1}{V_{max}}$ , where  $V$  is the initial velocity and  $[C]$  is the substrate concentration (Zhuang et al., 2003).

### 2.9. Identifying and quantifying TBP and its metabolites

The concentrations of TBP and intermediates in the enzyme mixture were analyzed using HPLC (Agilent1200 series) equipped with a DAD detector ( $\lambda = 230$  nm) (Zu et al., 2012). The TBP concentration was determined based on the chromatographic peak area ratio relative to individual standard calibration curves. The TBP metabolites generated by the dehalogenase were identified using gas chromatography (GC, Agilent 7890)-mass spectrometer (MS, Agilent 5975C) with and without N,O-bis(trimethylsilyl)-trifluoroacetamide (BSTFA) derivatization using a DB-5 column (30 m × 0.25 mm). The detailed extraction, evaporation, dissolution, and detection procedures and conditions were based on a previous study (Chen et al., 2011) and are provided in SI.

The evolution of Br<sup>-</sup> concentrations during the dehalogenation process was determined using the Metrohm 761 Compact IC ion chromatograph equipped with a Metrosep A SUPP 5250 (4 mm × 250 mm) column. Aliquots of 3.2 mM Na<sub>2</sub>CO<sub>3</sub> and 1.0 mM NaHCO<sub>3</sub> were used as the eluent, with a 0.7 mL min<sup>-1</sup> flow rate.

## 3. Results

### 3.1. Enzyme purification

The dehalogenase to support TBP degradation was extracted from the GZT strain by isolating cells from a culture grown using TBP as the sole carbon and energy source. As Fig. 1 shows, almost all of the dehalogenase activity of the strain GZT was associated with intracellular fraction after cell lysate centrifugation. No TBP debromination was observed in the membrane and extracellular fractions. This indicated that the target dehalogenase was an

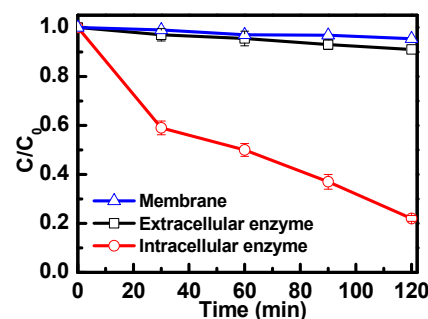


Fig. 1. Debromination of TBP by different subcellular fractions of *Bacillus* sp. GZT. C<sub>0</sub> and C were the TBP concentration at the initial time and time indicated, respectively.

intracellular enzyme.

The TBP dehalogenase was purified by monitoring TBP biodegradation. Purifying the TBP dehalogenase in the intracellular fraction consisted of five steps, including crude extract preparation, ammonium sulfate precipitation, DEAE-cellulose, and gel-filtration. As Fig. 2 lane 2 shows, two bands (one predominant band with approximately 65 kDa and one faint band with approximately 60 kDa) with one TBP-degrading activity peak (Fig. S1a) were found in the intracellular fraction after DEAE-cellulose chromatography purification. This suggested the need to further purify the TBP dehalogenase using other techniques. The subsequent purification by the Sephadex G-150 chromatography column resulted in the further increase of TBP dehalogenase activity (Table S1).

SDS-PAGE was used to identify one band with a molecular mass estimated as 63.4 kDa after subsequent purification (Fig. 2 lane 3). This indicated that the dehalogenase was homogenous, consisting of one polypeptide. Table S1 summarizes the results of TBP dehalogenase during typical enzyme purification. A total of 47-fold purification of dehalogenase relative to the crude cell extract was achieved. The specific TBP dehalogenase activity increased from 0.4 to 18.8 U mg<sup>-1</sup> of protein as the purification progress. Approximately 28.6% of the activity of TBP dehalogenase in the crude enzyme was recovered after the four treatment steps. Further, the enzyme stability test revealed that the purified dehalogenase could be stored at -20 °C for six months without a drop in activity (data not shown).

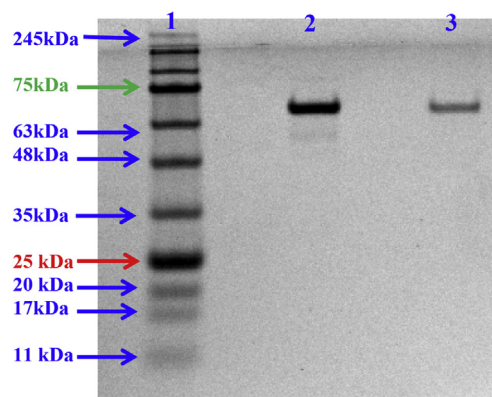


Fig. 2. SDS-PAGE analysis of the enzyme preparation from *Bacillus* sp. GZT. Lane 1, molecular size (kDa) marker; Lane 2, the fraction after DEAE-cellulose chromatography column; Lane 3, purified TBP dehalogenase after Sephadex G-150 chromatography column.

### 3.2. Biochemical characterization of TBP dehalogenase

The effects of temperatures and pH on TBP debromination activity by the purified dehalogenase and dehalogenase stability were firstly investigated. As Fig. S2a shows, the optimal temperature of the debrominating activity was 35 °C; higher and lower temperatures did not significantly support enzyme activity. The enzymatic system was stable under the assay conditions at temperatures below 40 °C for at least 2 h. Enzyme stability rapidly declined when the temperatures exceeded 35 °C.

With respect to pH, the initial TBP debromination efficiency was higher at a pH between 6.5 and 7.0 (Fig. S2b) and the optimum pH was 6.5. Pre-incubating the enzyme at different pH values, followed by the activity assay under standard conditions, resulted in enzyme stability in a pH range of 6.5–7.5. This stability declined rapidly at pH values greater than 8.0 or less than 6.0.

The effect of chemical reagents on TBP debromination by the purified dehalogenase was also investigated. Fig. 3 shows that debrominating activity was strongly inhibited by EDTA, methyl viologen, Ni<sup>2+</sup>, Cu<sup>2+</sup>, Ca<sup>2+</sup> and Fe<sup>2+</sup>. No significant effect was seen when adding glutathione and Zn<sup>2+</sup>. Adding H<sub>2</sub>O<sub>2</sub>, NADPH, Mn<sup>2+</sup> and Mg<sup>2+</sup> to the standard assay enzyme mixture efficiently promoted enzyme reactions.

Table 1 presents the substrate specificity of the purified enzyme towards different bromophenols. The debromination activity of TBP was set at a baseline of 100%. Compared to that, the highest debromination activity (143%) was observed for 2-BP. Debromination monobromophenol at the para- and meta-position (3-BP and 4-BP) were also found, but the activity was much lower. The specific activity of the enzyme towards 2,4-DBP was much higher than 2,6-DBP. However, no debromination activity was detected, either with 1,3-dibromo-2-methoxy-5-methylbenzene or 2,6-dibromo-4-methylphenol.

Kinetics parameters of obtained enzyme for TBP revealed that purified TBP dehalogenase showed a typical Michaelis-Menten profile. The apparent *K<sub>m</sub>* value of TBP was 78 μM, and *V<sub>max</sub>* was 0.65 μM min<sup>-1</sup> (mg protein<sup>-1</sup>) for TBP (Fig. S3).

### 3.3. Identifying the TBP dehalogenase with MALDI-TOF/TOF mass spectrometry

Table S2 and Fig. S4a show the protein homologs components generated from the tryptic digestion of purified enzyme excised from the gel bands. The MS/MS analysis of the 2005.98 peak identified the substance as a modified QVLNLTESQEIPMSDSAK

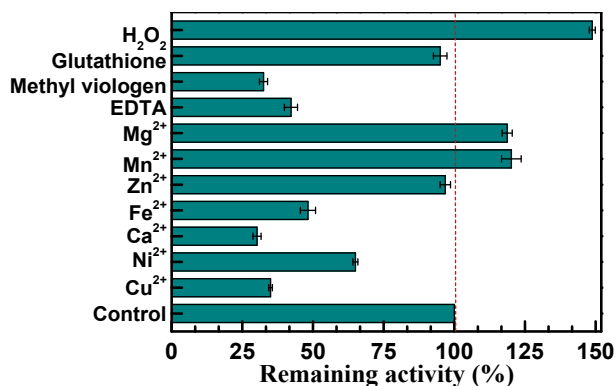


Fig. 3. The effect of different chemical reagents on TBP debromination by purified dehalogenase (Error bars represent standard deviations of duplicate results).

Table 1

Substrate specificity profile of TBP dehalogenase. Activities are expressed as the percentages of the rate found with TBP (Results are the means of triplicate measures).

Substrate	Relative activity (%)
2,4,6-Tribromophenol	100 ± 2.1
2,4-Dibromophenol	139 ± 3.5
2,6-Dibromophenol	123 ± 1.5
Benzoic acid	102 ± 4.6
2,6-Dibromo-4-methylphenol	ND <sup>a</sup>
1,3-Dibromo-2-methoxy-5-methylbenzene	ND <sup>a</sup>
2-Bromophenol	143 ± 3.3
Phenylacetic acid	112 ± 4.8
Phenol	97 ± 2.0
4-Bromophenol	66 ± 1.8
3-Bromophenol	55 ± 2.7

<sup>a</sup> Non-detected.

peptide. This corresponded to residues 53–70 of purified enzyme (theoretical *m/z* 2004.97). The ion score of 63 in the Mascot search revealed it to be TBP dehalogenase (*p* < 0.05) with the oligopeptide-binding protein and substrate-binding protein. Computer database matching resulted in a score of 807 for the purified protein with a sequence coverage of 39% of the total amino acids. Based on the sequence alignment analysis of the halo dehalogenase (Fig. S4b), it shared 98% identity to peptide ABC transporter substrate-binding protein from *Bacillus cereus*. Thus, the TBP dehalogenase differed from haloacid or reductive halogenase.

### 3.4. Gene cloning of TBP dehalogenase

The whole-genome sequence (accession no. LJVJ0000000) (Liang et al., 2016) available for *Bacillus* sp. GZT was screened with the ABC transporter protein sequences. This allowed us to find one closely linked open reading frame, namely ORF05005 (Table S3). This ORF coding peptide ABC transporter substrate-binding protein, was predicted to involve in the degradation pathway of TBP. To ensure determination of the gene sequence coding TBP dehalogenase, the corresponding ORF from strain GZT genomic DNA was also amplified and the resulting PCR amplicon was cloned yielding pET30-*tbp* plasmid. The results in Fig. S5 showed that a 565 bp fragment was successfully amplified. Sequence analysis of the insert DNA in the recombinant plasmid revealed that no PCR error has occurred. After the recombinant plasmid was introduced into *E. coli* and expressed, the functional recombinant strain with the ability to use TBP as carbon and energy source was selected. As shown in Fig. S6, although the negative control clone carrying an empty pET30a (+) disabled to survive on the TBP-containing plate, recombinant strains *E. coli* pET30-*tbp*, which can successfully growth and enrich on this plate, was regarded as the target recombinant strains carrying the TBP-degrading gene. Sequencing analysis of the recombinant plasmid showed that the target gene has been correctly and successfully introduced into the expression vector. SDS-PAGE (Fig. S7) analysis revealed one corresponding clear band with a molecular mass estimated at 31.7 kDa. This value is almost two times of the theoretical molecular mass, indicating that TBP dehalogenase is a dimeric protein.

### 3.5. Products analysis and mechanism prediction

To identify the purified enzyme's TBP biodegradation pathways under aerobic conditions, GC-MS was used to identify the degradation intermediates with or without BSTFA derivatization (Fig. S8).

Table S4 lists the intermediates associated with their chemical structures and the mass spectra. The  $m/z$  values of 194 and 208 corresponding to the  $M^+$  fragment were identified as the derivative products of benzoic acid (retention time (RT) = 12.654 min) and penylacetic acid (RT = 13.498 min), respectively. Validation with authentic standards revealed an additional two intermediates with the same  $m/z$  values but with slightly different RTs. These were identified as 2,4-DBP (RT = 14.252 min) and 2,6-DBP (RT = 14.719 min).

To further evaluate the degree of TBP biodegradation by the TBP dehalogenase, the concentration transition trend of above four intermediates and  $Br^-$  were also quantitatively analyzed. Fig. 4 shows that as the TBP concentration declined from 12.0 to 2.5  $\mu M$ , both dibromophenol intermediates reached their highest concentration at 60 min. The 2,4-DBP concentration was consistently higher than 2,6-DBP during the biodegradation tests. This suggests that the enzyme's initial biodegradation of TBP may be mainly through losing a Br atom at the TBP ortho position.

Although, no monobromophenol and phenol were detected, benzoic acid and penylacetic acid were gradually produced as the TBP biodegraded further and the dibromophenol intermediates identified above accumulated (Fig. 4a). As the operation time increased from 30 to 120 min, the accumulated bromide swiftly increased from 8 to 26  $\mu M$  (Fig. 4b). This further indicated that debromination is the primary way for the dehalogenase to metabolize TBP with  $Br^-$  generated as a final product.

Based on the intermediates identified above, the evolution curves, and published references, the metabolism mechanism of TBP by this dehalogenase was also proposed (Fig. 5). Three bromine atoms on the TBP molecule were substituted in a stepwise progression. The first step of the reaction is producing 2,4-DBP and 2,6-DBP by removing either an ortho or para bromine atom. Due to the 2,4-DBP concentration detected was higher than 2,6-DBP, the removal of ortho-substituted bromines may be preferential to para debromination. Then, these two dibromophenol products were further metabolized into benzoic acid and penylacetic acid. This is

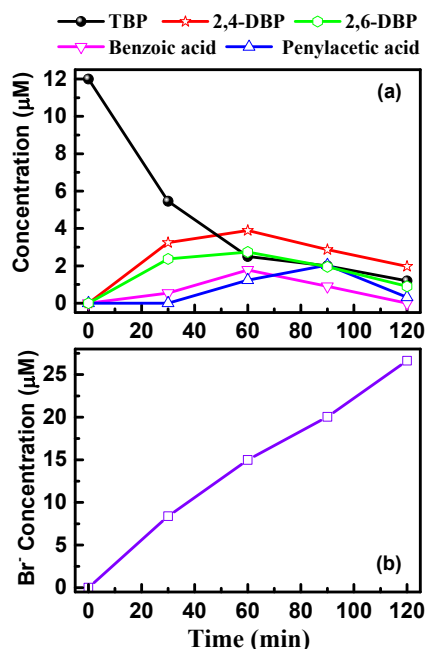


Fig. 4. Evolution curves of TBP biodegradation intermediates identified by GC-MSD analysis as well as bromide concentration versus the degradation time.

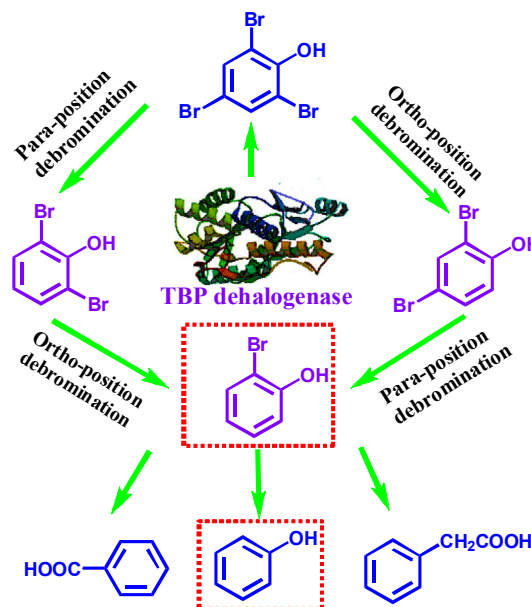


Fig. 5. Proposed TBP metabolic pathway by the TBP dehalogenase (Metabolites not identified in enzyme mixture are highlighted by red dashed lines). (For interpretation of the references to colour in this figure legend, the reader is referred to the web version of this article.)

done through 2-BP, which sequentially dehalogenates two bromine atoms. Although 2-BP was not detected in the GC-MS analysis, there was significant activity towards 2-BP when it was used as a sole substrate. The additional evidence supporting this hypothesis is the appearance of 2-BP during the metabolism of TBP by the GZT strain (Zu et al., 2012) and Raney Al-Ni alloy (Weidlich et al., 2013). The 2-BP may be absent because it is quickly transformed by bromophenol dehalogenase. Although, phenol was not detected during the degradation process due to low concentration, other studies have identified phenol to be the dehalogenation product of TBP (Ronen et al., 2000; Yamada et al., 2008), which suggests that the dehalogenase could metabolize the TBP into phenol. This pathway coincides with the reductive debromination process mediated by TBP biodegradation strain, with the exception of the methylation pathway. This further confirms that this dehalogenase originated from the GZT strain.

#### 4. Discussion

Microbes survived in the xenobiotics contaminated sites, apparently having evolved to remove naturally occurring or synthetic halogenated compounds in order either to exploit them as a carbon source for growth or as a means of protection strategy against the toxicity of these compounds (Sfetsas et al., 2009). Dehalogenation is a common first and critical step in degrading halogenated compounds, because products with fewer halogen substituents are more susceptible to aerobic biodegradation (Chen et al., 2013; Wang et al., 2010). Generally, DHAs catalyze the detoxification of halogenated aromatics by replacing the halogen with other atoms, like hydrogen (Bisaillon et al., 2010).

To date, although several DHAs purified from chlorinated compounds degrading bacteria have been reported, only two previous studies have focused on the dehalogenase of brominated aromatics (Chen et al., 2013; Yang et al., 2015). Thus, the TBP dehalogenase purified and characterized by this study will further improve our understanding of enzyme catalysis process contributing to

brominated aromatics attenuation at contaminated sites. Although most reported RDases are usually membrane-associated and oxygen sensitive enzymes (Boyer et al., 2003; Payne et al., 2015), the dehalogenase activity in the GZT strain was mainly located in the intracellular fraction under aerobic conditions. This result aligns with the identification of haloacid and tetrachloroethene DHAs in *P. stutzeri* DEH130 and *S. sediminis*, respectively (Lohner and Spormann, 2013; Zhang et al., 2013). Different DHAs have some common features. For example, they share an optimal pH range of 6.5–7.5 (Zhang et al., 2013). We found that the GZT strain achieved higher degradation and debromination efficiencies in this same pH range (Zu et al., 2012). The optimum pH was also determined to be 7.0 and 6.5 for trichlorophenol and 3-chloro-4-hydroxybenzoate from *D. frapperi* PCP-1 and *D. chlororespirans* Co23, respectively (Boyer et al., 2003).

Other factors are critical in applying dehalogenase remediation to address environmental contaminants. For example, in this study, dehalogenase activity was inhibited by adding  $\text{Cu}^{2+}$ , EDTA,  $\text{Ni}^{2+}$ ,  $\text{Ca}^{2+}$  and  $\text{Fe}^{2+}$ . Other dehalogenases have been shown to be sensitive to some of these metal ions, or other ions such as  $\text{Co}^{2+}$ ,  $\text{Hg}^{2+}$  and  $\text{Ag}^+$ . The extent of sensitivity is related to the enzyme source (Xue et al., 2014; Zhang et al., 2013).  $\text{Zn}^{2+}$  did not inhibit TBP dehalogenase, a finding consistent with results associated with trichlorophenol dehalogenase (Boyer et al., 2003). The cofactor NADPH greatly increased purified enzyme activity. This finding was similar to other research focusing on bromoxynil dehalogenase (Chen et al., 2013) and pentachlorophenol monooxygenase (Camacho-Perez et al., 2012).

Fig. 2 shows that the purified dehalogenase has an apparent molecular mass of 63.4 kDa. This value falls within the range of the molecular mass (40–65 kDa) determined for RDases (Thibodeau et al., 2004), but differs from the brominated aromatic reductive dehalogenase of *Comamonas* sp. 7D-2 (117.9 kDa) (Chen et al., 2013), which is approximately twice as large as our dehalogenase. It also differs from 2-haloacid dehalogenase, which has two subunits (Zhang et al., 2014). One possible explanation for this result is that different types of dehalogenases are composed of various amino acids coded by non-identical genes, yielding different sizes (Zhou et al., 2004).

Significantly, the TBP dehalogenase activity was higher than some known TBP-degrading strains, such as the TB01 strain (Yamada et al., 2008) and the GZT strain (Zu et al., 2012). The purified enzyme degraded 80% of the TBP in a short time (120 min). The estimated  $K_m$  of the dehalogenase for TBP was 78  $\mu\text{M}$ , which is less than other dehalogenases, such as haloalkane and tetrachloroethene dehalogenase (Kumar et al., 2014; Lohner and Spormann, 2013). This suggests that the TBP dehalogenase might have a high affinity to TBP. As predicted from the alignment with the related sequences in the RAST database, the genome sequences in the GZT strain are very similar to *Bacillus cereus* (Liang et al., 2016). Further, it was found that genus *Bacillus cereus* contained phosphonate, a member of the haloacid dehalogenase superfamily (Lahiri et al., 2006). However, according to the sequence alignment analysis result, the TBP dehalogenase's sequence is similar to the peptide ABC transporter substrate-binding protein. Moreover, TBP dehalogenase activity of the transformation product was also confirmed by cloning and expression of the gene encoding this enzyme into *E. coli*. The above information suggested that this enzyme produced by the GZT strain may be a novel dehalogenase.

The substrate spectrum of the purified enzyme was similar to our previous report for *Bacillus* sp. GZT, indicating that the dehalogenase obtained here is the main enzyme involved in TBP dehalogenating. The substances 2,6-dibromo-4-methylphenol and 1,3-dibromo-2-methoxy can both be degraded by the GZT strain; however, neither could serve as a substrate for the purified TBP

dehalogenase. This suggests that, in addition to the new dehalogenase, the GZT strain may also have other enzyme systems. Further, the purified enzyme may not belong to S-adenosyl-L-methionine-dependent methyltransferase catalyzed O-methylation.

In addition, higher concentration of 2,4-DBP than 2,6-DBP, suggested that the debromination of *ortho*-halophenol was faster than that of *para*-halophenols. This result was consistent with previous research focusing on TBP debromination by the GZT strain (Zu et al., 2012), Raney Al-Ni alloy (Weidlich et al., 2013), *Ochrobactrum* sp. strain TB01 (Yamada et al., 2008) and a marine sponge (Ahn et al., 2003). Moreover, higher degradation activity in 2-BP than 3-BP and 4-BP indicated that *ortho*-position bromophenol removal precedes *para*- and *meta*-position bromophenol removal. This may be resulted from the dehalogenase's interaction with the compound interfered with steric hindrance (Yamada et al., 2008), which is consistent with a previous study (Ahn et al., 2003). Further, the TBP dehalogenase biodegradation mechanism is similar to TBP debromination by the GZT strain (Zu et al., 2012). This suggests that this dehalogenase is the major enzyme system in the GZT strain.

This finding, along with the high specific activity in cell extracts and the low apparent  $K_m$  of TBP of the purified enzyme, leads to the conclusion that TBP dehalogenase is a specific enzyme highly suited for debrominating TBP. This is surprising, as these compounds are xenobiotics and remain in the environment at significance concentrations for a long time. Our study identified this excellent dehalogenase candidate for further application in green chemistry and the environment; it also offers new information about an environmentally important *Bacillus*-type TBP dehalogenase.

## 5. Conclusion

This study successfully identified and isolated a novel TBP dehalogenase from *Bacillus* sp. GZT. Biochemical characterization suggested that the enzyme is both thermo- and pH-stable, and the enzyme can efficiently debrominate TBP. This is the first biochemical report to unambiguously demonstrate the existence of a TBP dehalogenase under aerobic condition. These findings have significant implications for the future remediation of TBP-contaminated sites.

## Conflict of interests

There is no conflict of interests.

## Acknowledgments

This work was financially supported by NSFC (41373103 and 41573086), National Natural Science Funds for Distinguished Young Scholars (41425015).

## Appendix A. Supplementary data

Supplementary data related to this article can be found at <http://dx.doi.org/10.1016/j.envpol.2017.03.043>.

## References

- Ahn, Y.B., Rhee, S.K., Fennell, D.E., Kerkhof, L.J., Hentschel, U., Haggblom, M.M., 2003. Reductive dehalogenation of brominated phenolic compounds by microorganisms associated with the marine sponge *Aplysina aerophoba*. *Appl. Environ. Microbiol.* 69, 4159–4166.
- Arora, P.K., Bae, H., 2014. Role of dehalogenases in aerobic bacterial degradation of chlorinated aromatic compounds. *J. Chem.* 2014. Article ID 157974, 10 pages. <http://dx.doi.org/10.1155/2014/157974>.

- Bisaillon, A., Beaudet, R., Lepine, F., Deziel, E., Villemur, R., 2010. Identification and characterization of a novel CprA reductive dehalogenase specific to highly chlorinated phenols from *Desulfotobacterium hafniense* strain PCP-1. *Appl. Environ. Microbiol.* 76, 7536–7540.
- Boyer, A., Page-Belanger, R., Saucier, M., Villemur, R., Lepine, F., Juteau, P., Beaudet, R., 2003. Purification, cloning and sequencing of an enzyme mediating the reductive dechlorination of 2,4,6-trichlorophenol from *Desulfotobacterium frappieri* PCP-1. *Biochem. J.* 373, 297–303.
- Camacho-Perez, B., Rios-Leal, E., Rinderknecht-Seijas, N., Poggi-Valardo, H.M., 2012. Enzymes involved in the biodegradation of hexachlorocyclohexane: a mini review. *J. Environ. Manage* 95, S306–S318.
- Chen, D.H., Bi, X.H., Liu, M., Huang, B., Sheng, G.Y., Fu, J.M., 2011. Phase partitioning, concentration variation and risk assessment of polybrominated diphenyl ethers (PBDEs) in the atmosphere of an e-waste recycling site. *Chemosphere* 82, 1246–1252.
- Chen, K., Huang, L.L., Xu, C.F., Liu, X.M., He, J., Zinder, S.H., Li, S.P., Jiang, J.D., 2013. Molecular characterization of the enzymes involved in the degradation of a brominated aromatic herbicide. *Mol. Microbiol.* 89, 1121–1139.
- Chow, W.L., Cheng, D., Wang, S.Q., He, J.Z., 2010. Identification and transcriptional analysis of trans-DCE-producing reductive dehalogenases in *Dehalococcoides* species. *ISME J.* 4, 1020–1030.
- Contreras, D., Oviedo, C., Valenzuela, R., Freer, J., Rojo, K., Rodriguez, J., 2009. Tri-bromophenol degradation by a catechol-driven fenton reaction. *J. Chil. Chem. Soc.* 54, 141–143.
- Donoso, C., Becerra, J., Martinez, M., Garrido, N., Silva, M., 2008. Degradative ability of 2,4,6-tribromophenol by saprophytic fungi *Trametes versicolor* and *Agaricus augustus* isolated from Chilean forestry. *World J. Microbiol. Biotechnol.* 24, 961–968.
- Ezechias, M., Covino, S., Cajthaml, T., 2014. Ecotoxicity and biodegradability of new brominated flame retardants: a review. *Ecotoxicol. Environ. Safe* 110, 153–167.
- Futagami, T., Goto, M., Furukawa, K., 2008. Biochemical and genetic bases of dehalorespiration. *Chem. Rec.* 8, 1–12.
- Janssen, D.B., Dinkla, I.J.T., Poelarends, G.J., Terpstra, P., 2005. Bacterial degradation of xenobiotic compounds: evolution and distribution of novel enzyme activities. *Environ. Microbiol.* 7, 1868–1882.
- Jugder, B.E., Ertan, H., Bohl, S., Lee, M., Marquis, C.P., Manefield, M., 2016. Organohalide respiring bacteria and reductive dehalogenases: key tools in organohalide bioremediation. *Front. Microbiol.* 7, 249.
- Karigar, C.S., Rao, S.S., 2011. Role of microbial enzymes in the bioremediation of pollutants: a review. *Enzyme Res.* 2011, 805187.
- Kumar, A., Pillay, B., Olaniran, A.O., 2014. Cloning, expression, purification and three-dimensional structure prediction of haloalkane dehalogenase from a recently isolated *Ancylobacter aquaticus* strain UV5. *Protein Expr. Purif.* 99, 10–17.
- Laemmli, U., 1970. Cleavage of structural proteins during the assembly of the head of bacteriophage T4. *Nature* 227, 680–685.
- Lahiri, S.D., Zhang, G.F., Dunaway-Mariano, D., Allen, K.N., 2006. Diversification of function in the haloacid dehalogenase enzyme superfamily: the role of the cap domain in hydrolytic phosphorus-carbon bond cleavage. *Bioorg. Chem.* 34, 394–409.
- Li, Z.L., Yoshida, N., Wang, A.J., Nan, J., Liang, B., Zhang, C.F., Zhang, D.D., Suzuki, D., Zhou, X., Xiao, Z.X., Katayama, A., 2015. Anaerobic mineralization of 2,4,6-tribromophenol to CO<sub>2</sub> by a synthetic microbial community comprising *Clostridium*, *Dehalobacter*, and *Desulfatigibans*. *Bioresour. Technol.* 176, 225–232.
- Liang, Z.S., Li, G.Y., An, T.C., Das, R.J., 2016. Draft genome sequence of *Bacillus* sp. GZT, a 2,4,6-tribromophenol degrading strain isolated from the river sludge of an electronic waste-dismantling region. *Genome Announc.* 4 <http://dx.doi.org/10.1128/genomeA.00474-16>.
- Lohner, S.T., Spormann, A.M., 2013. Identification of a reductive tetrachloroethene dehalogenase in *Shewanella sediminis*. *Philos. Trans. R. Soc. B-B* 368. <http://dx.doi.org/10.1098/rstb.2012.0326>.
- Luo, S., Yang, S.G., Sun, C., Wang, X.D., 2011. Feasibility of a two-stage reduction/subsequent oxidation for treating Tetrabromobisphenol A in aqueous solutions. *Water Res.* 45, 1519–1528.
- Modaressi, K., Taylor, K.E., Bewtra, J.K., Biswas, N., 2005. Laccase-catalyzed removal of bisphenol-A from water: protective effect of PEG on enzyme activity. *Water Res.* 39, 4309–4316.
- Morris, R.M., Fung, J.M., Rahm, B.G., Zhang, S., Freedman, D.L., Zinder, S.H., Richardson, R.E., 2007. Comparative proteomics of *Dehalococcoides* spp. reveals strain-specific peptides associated with activity. *Appl. Environ. Microbiol.* 73, 320–326.
- Ni, S.S., Fredrickson, J.K., Xun, L.Y., 1995. Purification and characterization of a novel 3-chlorobenzoate-reductive dehalogenase from the cytoplasmic membrane of *Desulfomonile-Tiedjei* Dcb-1. *J. Bacteriol.* 177, 5135–5139.
- Parthasarathy, A., Stich, T.A., Lohner, S.T., Lesnfsky, A., Britt, R.D., Spormann, A.M., 2015. Biochemical and EPR-spectroscopic investigation into heterologously expressed vinyl chloride reductive dehalogenase (Vcra) from *Dehalococcoides mccartyi* Strain VS. *J. Am. Chem. Soc.* 137, 3525–3532.
- Payne, K.A.P., Quezada, C.P., Fisher, K., Dunstan, M.S., Collins, F.A., Sjuts, H., Levy, C., Hay, S., Rigby, S.E.J., Leys, D., 2015. Reductive dehalogenase structure suggests a mechanism for B12-dependent dehalogenation. *Nature* 517, 513–516.
- Ronen, Z., Vasiluk, L., Abeliovich, A., Nejidat, A., 2000. Activity and survival of tribromophenol-degrading bacteria in a contaminated desert soil. *Soil Biol. Biochem.* 32, 1643–1650.
- Schmidt, M., Lege, S., Nijenhuis, I., 2014. Comparison of 1,2-dichloroethane, dichloroethene and vinyl chloride carbon stable isotope fractionation during dechlorination by two *Dehalococcoides* strains. *Water Res.* 52, 146–154.
- Sfetsas, C.C., Miliotis, L., Skopelitou, K., Venieraki, A., Todou, R., Fletmetakis, E., Katinakis, P., Labrou, N.E., 2009. Characterization of 1,2-dibromoethane-degrading haloalkane dehalogenase from *Bradyrhizobium japonicum* USDA110. *Enzyme Microb. Technol.* 45, 397–404.
- Su, J.M., Deng, L., Huang, L.B., Guo, S.J., Liu, F., He, J., 2014. Catalytic oxidation of manganese(II) by multicopper oxidase CueO and characterization of the biogenic Mn oxide. *Water Res.* 56, 304–313.
- Thibodeau, J., Gauthier, A., Duguay, M., Villemur, R., Lepine, F., Juteau, P., Beaudet, R., 2004. Purification, cloning, and sequencing of a 3,5-dichlorophenol reductive dehalogenase from *Desulfotobacterium frappieri* PCP-1. *Appl. Environ. Microbiol.* 70, 4532–4537.
- Thomsen, C., Lundanes, E., Becher, G., 2001. Brominated flame retardants in plasma samples from three different occupational groups in Norway. *J. Environ. Monit.* 3, 366–370.
- Travkin, V.M., Linko, E.V., Golovleva, L.A., 1999. Purification and characterization of maleylacetate reductase from *Nocardioideis simplex* 3E utilizing phenoxyalcanoic herbicides 2,4-d and 2,4,5-T. *Biochem.-Moscov* 64, 625–630.
- Uhnakova, B., Petrickova, A., Biedermann, D., Homolka, L., Vejvoda, V., Bednar, P., Papouškova, B., Sulc, M., Martinkova, L., 2009. Biodegradation of brominated aromatics by cultures and laccase of *Trametes versicolor*. *Chemosphere* 76, 826–832.
- Wang, G.L., Li, R., Li, S.P., Jiang, J.D., 2010. A novel hydrolytic dehalogenase for the chlorinated aromatic compound chloroethanol. *J. Bacteriol.* 192, 2737–2745.
- Weidlich, T., Prokes, L., Pospisilova, D., 2013. Debromination of 2,4,6-tribromophenol coupled with biodegradation. *Cent. Eur. J. Chem.* 11, 979–987.
- Xiong, J., Li, G.Y., An, T.C., Zhang, C.S., Wei, C.H., 2016. Emission patterns and risk assessment of polybrominated diphenyl ethers and bromophenols in water and sediments from the Beijiing River, South China. *Environ. Pollut.* 219, 596–603.
- Xue, F., Liu, Z.Q., Wan, N.W., Zheng, Y.G., 2014. Purification, gene cloning, and characterization of a novel haloalohydrin dehalogenase from *Agromyces mediolanus* ZJB120203. *Appl. Biochem. Biotechnol.* 174, 352–364.
- Yamada, T., Takahama, Y., Yamada, Y., 2008. Biodegradation of 2,4,6-tribromophenol by *Ochrobactrum* sp strain TB01. *Biosci. Biotechnol. Biochem.* 72, 1264–1271.
- Yang, C., Kublik, A., Weidauer, C., Seiwert, B., Adrian, L., 2015. Reductive dehalogenation of oligocyclic phenolic bromoaromatics by *Dehalococcoides mccartyi* strain CBDB1. *Environ. Sci. Technol.* 49, 8497–8505.
- Zhang, J.Y., Cao, X.P., Xin, Y.J., Xue, S., Zhang, W., 2013. Purification and characterization of a dehalogenase from *Pseudomonas stutzeri* DEH130 isolated from the marine sponge *Hymeniacidon perlevis*. *World J. Microbiol. Biotechnol.* 29, 1791–1799.
- Zhang, J.Y., Xin, Y.J., Cao, X.P., Xue, S., Zhang, W., 2014. Purification and characterization of 2-haloacid dehalogenase from marine bacterium *Paracoccus* sp DEH99, isolated from marine sponge *Hymeniacidon perlevis*. *J. Ocean. U. China* 13, 91–96.
- Zhou, L.H., Marks, T.S., Poh, R.P.C., Smith, R.J., Chowdhry, B.Z., Smith, A.R.W., 2004. The purification and characterisation of 4-chlorobenzoate: CoA ligase and 4-chlorobenzoyl CoA dehalogenase from *Arthrobacter* sp strain TM-1. *Biodegradation* 15, 97–109.
- Zhuang, Z.H., Gartemann, K.H., Eichenlaub, R., Dunaway-Mariano, D., 2003. Characterization of the 4-hydroxybenzoyl-coenzyme A thioesterase from *Arthrobacter* sp strain SU. *Appl. Environ. Microbiol.* 69, 2707–2711.
- Zu, L., Li, G.Y., An, J.B., Li, J.J., An, T.C., 2013. Kinetic optimization of biodegradation and debromination of 2,4,6-tribromophenol using response surface methodology. *Int. Biodeter. Biodegr* 76, 18–23.
- Zu, L., Li, G.Y., An, T.C., Wong, P.K., 2012. Biodegradation kinetics and mechanism of 2,4,6-tribromophenol by *Bacillus* sp GZT: a phenomenon of xenobiotic methylation during debromination. *Bioresour. Technol.* 110, 153–159.